Vehicular Communications 38 (2022) 100534

Contents lists available at ScienceDirect

Vehicular Communications

journal homepage: www.elsevier.com/locate/vehcom

A multi-layer probing approach for video over 5G in vehicular scenarios

Rui Lopes [a,b,*], Filipe Rocha [a], Susana Sargento [a,b], Miguel Luís [b,c], Ricardo Leitão [d], Eduardo Marques [d], Bruno Antunes [d]

[a] *Departamento de Eletrónica, Telecomunicações e Informática, Universidade de Aveiro, 3810-193 Aveiro, Portugal*
[b] *Instituto de Telecomunicações, 3810-193 Aveiro, Portugal*
[c] *ISEL - Instituto Superior de Engenharia de Lisboa, 1959-007 Lisboa, Portugal*
[d] *Wavecom Engineering, 3800-125 Aveiro, Portugal*

ARTICLE INFO

Article history:
Received 6 May 2022
Received in revised form 19 September 2022
Accepted 7 October 2022
Available online 12 October 2022

Keywords:
Video transmission
5G
MPEG-DASH
Key performance indicators (KPIs)
Mobile networks

ABSTRACT

Fifth generation (5G) technologies are becoming a reality throughout the world. In parallel, vehicular networks rise their pace in terms of utilization; moreover, multimedia content transmissions are also getting an always increasing demand by their users. Besides the promised performance of 5G networks, several questions still arise among the community: are these networks capable of delivering high quality video streaming services in moving scenarios? What is the relationship between the network conditions and the video quality of experience?

To answer to the previous questions, in this paper we propose a multi-layer probing approach able to assess video transmissions over 5G and 4G, combining data from all layers of a communication model, relating events from its origin layers. The probe's potential is thoroughly evaluated in two distinct video streaming use cases, both targeting a vehicular scenario supported by cellular 4G and 5G networks. Regarding the probe's performance, we show that a multitude of performance and quality indicators, from different stack layers, can be obtained. As for the performance of 4G and 5G networks in video streaming scenarios, the results have shown that the 5G links show a better overall performance in terms of video quality-of-experience, granting lower delays and jitter conditions, thus allowing video delay to be diminished and segment buffering to be better performed in comparison to 4G, while still showing adaptability in lightly traffic-saturated vehicular-to-vehicular scenarios.

1. Introduction

As 5G networks are gaining strong attention from the global population, following the promise of an high-quality service with low latency and high bandwidth, the number of devices connected to such a network is trending for an expected 10 percent of global mobile devices by 2023, as reported by Cisco in [1].

The trend in the usage and transmission of multimedia content has also increased, specifically regarding video streaming activities and applications where higher and more severe constraints are placed on network intermediates, due to the bitrates of the state-of-the-art ultra high definition (UHD) videos. For instance, as mentioned in [1], UHD video has a variable bitrate between 15 to 18 Mbps, which can be considered to be more than double the high definition (HD) video standard, and approximately nine times higher than standard definition (SD) video bitrate. This reasoning leads us to believe that it is critical to have tools to monitor and adequately assess such networks' performance in video transmission.

Several aspects should be considered regarding multimedia content (and video in specific) since this traffic profile is prone to error propagation during its transmission. Since it is to be perceived by users, a small error in the transmission can lead to artifacts on the screen, compromising the user's quality of experience (QoE). As defined by ETSI as the "overall acceptability of an application or service, as perceived subjectively by the end-user, [*also including*] the complete end-to-end system effects (client, terminal, network, services infrastructures, etc.)" [2], we can consider that it is not an easy task to provide a proper QoE, requiring, in order to be estimated, data from a wide array of metrics to assess such an indicator.

* Corresponding author.
E-mail addresses: ruieduardo.fa.lopes@ua.pt (R. Lopes), filipe.esr@ua.pt (F. Rocha), susana@ua.pt (S. Sargento), nmal@av.it.pt (M. Luís), rleitao@wavecom.pt (R. Leitão), emarques@wavecom.pt (E. Marques), bantunes@wavecom.pt (B. Antunes).

https://doi.org/10.1016/j.vehcom.2022.100534
2214-2096/

In this article, we propose a 5G performance compliance testing assurance solution that retrieves and estimates key performance indicators (KPIs) and key quality indicators (KQIs) to represent the natural and current behaviors of the 5G network and services, mainly focusing on the perceived multimedia quality over fourth generation (4G) and 5G vehicular scenarios. By developing a multi-layer probe with a client-centric monitoring approach [3], a mean opinion score (MOS) value can be assessed combining metrics from a cross-layer perspective and representing the performance of the transmitted service, as it is received from a 5G station.

The potential of the proposed approach is assessed under a real-world 5G mobile scenario, namely, a vehicular network where the end-user sits inside a vehicle, connected to the Internet through 5G. Then, two separate use cases are explored. In the first one, the end-user requests a video from a remote video server placed outside the 5G network context (in the cloud, for example). In the second use case, another end-user recorded the video in a different car as part of the 5G network context and sent it to the rear vehicle. This work then evaluates the performance of a 5G network and its ability to deliver high-definition multimedia content to its users in a mobile environment.

In summary, the main contributions of this article are as follows:

1. Evaluate the potential of the multi-layer probing mechanism, regarding the collection of metrics amongst the several layers of the communication stack;
2. Collect metrics in two video streaming scenarios (vehicle-to-infrastructure *versus* vehicle-to-vehicle), with different network conditions (line-of-sight *versus* non-light-of-sight), with different cellular standards (4G and 5G), and different saturation levels of the radio access technology;
3. Assess the performance of the probing mechanism regarding its capability of characterizing the network conditions and estimating the quality level of the video streaming under a given cellular technology.

The remaining of this document is organized as follows. Section 2 discusses the related work. Section 3 overviews the most important performance and quality key indicators concerning the communication network and video reproduction. Section 4 presents the global architecture of the proposed probing mechanism and details the implementation of the probing mechanism. Section 5 presents scenarios and tests, and Section 6 discusses the results. Finally, Section 7 enumerates the conclusions and directions for future work.

2. Related work

Several research works have already been developed to assess a network's (or a system's) performance under multimedia streaming scenarios. Since these works show a trend of taking considerable attention to QoE and provide different parameters on how to estimate its evaluations [4], in opposition to the solution hereby proposed, we also point out extensive work on other topics that we consider relevant to the overall streaming assessment.

Starting at a physical layer, radio metrics are usually obtained by averaging large-scale time range samples [5,6]. Several works were found to explore radio metrics and correlate them with others to obtain behavioral relations between indicators, trying to relate them with criteria of quality of service (QoS) and QoE. The work in [7] defines relations between metrics such as received signal strength indicator (RSSI) or signal-to-interference-noise ratio (SINR), in correlation with other parameters leading to mappings to certain levels of QoS, using Long Term Evolution (LTE). On the other hand, by using 5G networks, work is still under development to which a mapping between QoS and QoE concerns: in the works of Tikhvinskiy et al. in [8], Angelopoulos et al. in [9], and Banović-Ćurguz et al. in [10], one can see that similar works are in place. However, they still theoretically propose metrics that could not yet be experimented with due to the lack of testing infrastructure in most cases.

Bridging to the network layer of the standard communication stack, and as the impact of user-perceived QoE using multimedia services significantly relies on the QoS parameters, the authors in [11] support such statement by considering delay and packet loss rate as key QoS parameters to compute an opinion score. In real-time video streaming applications, generally, when a packet does not arrive within a specific and strict time slot, one should believe that it is lost, which will produce unwanted consequences to the user experience on the client devices. In this work, Mushtaq et al. propose an assessment and focus more attention on a video server selection attending to the video codec specifications provided to the clients, choosing proper bitrates depending on which can offer better QoE with a minimal overall network delay.

Also from a server's perspective, in work by Dubin et al. [12] requests made from a client are analyzed and content is retrieved based on the capability of the server to respond, attempting to maximize the user's QoE by providing content at a rhythm the server can respond, tackling its bottleneck issue. This approach does not get metrics from the client, but rather from its requests and trades the requests with its transmission capabilities regarding the connection's current status. In the same year, in 2019, in the work by Li [13], the impact of packet throughput while in a video transmission on the user QoE as it visualizes the content, as well as in a scenario where traffic crosses different autonomous systems, is studied. Here stating the results from a client perspective on the monitoring task, Li analyzed the causal relationship between throughput and user engagement, showing that effects rise with a larger impact on medium-to-long-length video views.

The latter works mainly use layer-3 metrics to process and infer QoE values. Other authors append layer-4 metrics and above to it, which is the case of the work by Mazhar et al. [14]. The authors proposed a method, by using machine learning techniques, to infer QoE metrics with network and transport layer inputs, such as network latencies or transport issues ultimately causing rebuffering events. This method, although not taking advantage of any physical or link-layer indicator, also takes into consideration the fact that most traffic nowadays is end-to-end encrypted, which makes difficult the visibility of the underlying traffic of a given network path.

By studying the trade-off between the possibility of adding start-up delay and content starvation to happen, Bouraqia et al. [15] produced simulations whose results validated the consideration of QoS metrics for both triggering and modification of the transmission of the packets to process features of start-up delay.

Song et al. in [16] also proposed a work focused on a user-centric objective QoE assessment, where a model is designed to estimate the user's overall QoE for audiovisual services. This model, taking into account perceptual audiovisual quality and user interest in the content being viewed, allows metrics to be raised from human-interaction aspects and distance themselves from technology-centric quality metrics that evaluate multimedia services.

In 2018, Nightingale et al. in [17], proposed a 5G-QoE framework which provides a QoE prediction model sufficiently accurate and of low complexity as a real-time indicator of video application flow status in ultra-high definition video flows within the context of 5G networks. Also focusing on a user-centric approach, this model was developed and evaluated through subjective experiments using over 50 human subjects against metrics captured from QoE indicators.

In [18], Lopez et al. presented a software module that can assess video quality when applied at a given point of a flow within a network to retrieve metrics on the link status. Although complemented with some QoS indicators, these metrics were also strongly coupled within the context of user-relatable indicators, such as video quality analysis of color errors or frozen frames.

Visualization errors can impact the quality of experience differently to the users depending on the type and how deep in the OSI layer the error occurs. Bhargava et al., in [19], studied the impact of errors in a buffer-based reception versus a capacity-based, which tries to provide the highest video quality possible but producing many artifacts during playback. This work is focused on the client-side, and the monitoring features are part of the MPEG Dynamic Adaptive Streaming over HTTP (MPEG-DASH) client controller used in this work, looking over some metrics such as video delay. Also, from the same perspective and framework, the work by Qiao et al. [20] uses three different QoE metrics to monitor the video content reception: the average bitrate, the number of bitrate switches, and the number of rebuffering events. The usage of these metrics was made to promote the quality of experience in an online fashion, which they implemented in the reference DASH client implementation *dash.js*.

Rising to a higher abstraction level towards the user experience in the visualization of a video, some works try to establish changes in how content is transmitted and shown, according to a user QoE estimation. Using an MPEG-DASH client controller, one of its features is the usage of an adaptive bit rate (ABR) algorithm to determine the optimal video playback quality. As a client can face unpredicted bandwidth changes due to transport, network, or physical issues, a proposed solution by Hou et al. [21] assumes these as something uncontrollable, and tries to optimize the content visualization in terms of the client resources with the help of a deep learning network technique. On the other hand, in the work by El Meligy et al. [22], not trying to balance the usage of a buffer-based or a capacity-based algorithm for ABR, they proposed a new buffer-based algorithm in which the bandwidth usage is improved by handling the occupancy of the client playback buffer around a given level, absorbing any undesirable network change below. Not being a monitoring project, it is a proposal of a new algorithm that monitors the playback buffer length to correlate with acceptable video quality and a low number of content representation level switches.

Getting closer to applications able to serve as clients to a video transmission, in [23] the authors provide a list of information obtained from measuring QoS parameters on LTE networks, on reaching services such as Facebook's or YouTube's, to assess the service QoE. Using machine learning approaches, they have prepared a model to assess a MOS value based on LTE usage. In another work, Bartolec et al. [24] studied the interactions a user can have with a video client player during the playback of content. Such interactions, such as pausing, seeking, abandoning the video playback, or changing the playback speed, are shown to impact the performance of models that estimate KPIs from encrypted traffic. Continuing this work, the proposal by Orsolic et al. in [25] studied YouTube's streaming sessions, in which metrics on the user's perception were being obtained was made varying the video contents and the location where clients were (different locations in Europe were chosen). From this study, it was revealed that performance metrics were shown to be degraded when models trained from one city's dataset were tested with others.

As mentioned in earlier works, the user experience is not only influenced by infrastructure, network, or transport issues, but also by context, human, and environmental factors, which are challenging to define in a global case. For this reason, Laiche et al. [26] have proposed a monitoring web application where users can visualize video content being transmitted, and subjective and objective KPIs are obtained from the system, human, context, and social-behavioral factors.

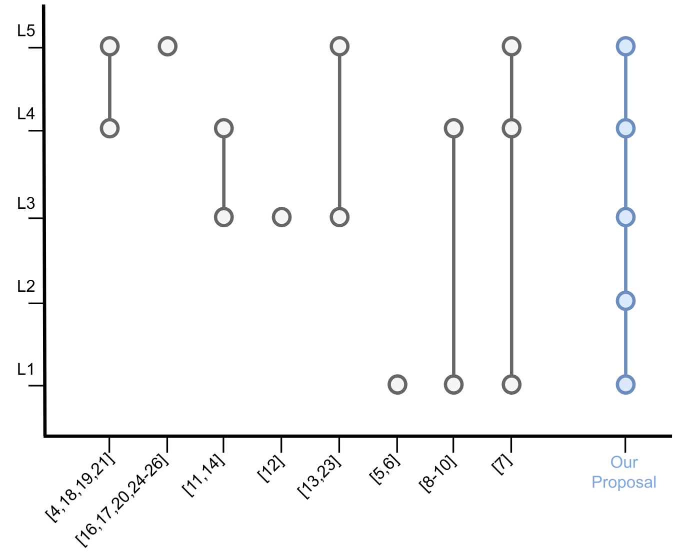

Fig. 1. Related works approaches for probing mechanism per communication layer, and our contribution.

All of these works contribute to orienting our work proposal: to gather metrics in each layer of the communication model, relate them, and conduct a global assessment of the experience of a video streaming session. Fig. 1 depicts our approach in comparison with the presented related work.

3. Performance and quality indicators

In a video transmission traversing multiple network links in a node-to-node 5G network, not only the video-related statistics are relevant, but the video flow's status also depends on the link's health in different network layers. Consequently, to estimate the status of a video transmission and the respective network performance, several indicators must be taken into account in each abstraction layer of a computer networking system. These indicators must then be acquired regarding network and access capabilities and the video transmission service.

3.1. Conceptualization

Once we mention network and access capabilities, then KPIs must be in place. These indicators, such as network latency, reliability, and availability, among other metrics, assess how the components from the infrastructure to the network are supporting a connection, independently of the current applications whose transmissions are being held.

The main KPIs for the vehicular multimedia scenarios can be described as follows [27,28]:

- Communication Range: the communication is highly influenced by the velocity of the mobile nodes;
- Network Latency: propagation and processing delays are inherent to the computer systems and connections made between the server and client machines;
- Availability: the percentage of the time a computer system is available to perform and maintain a connection stable as needed to run a video transmission over it;
- Reliability: an indicator given by the probability that the latency is lower or equal to the network latency variable.

The QoE assessment also requires that KQIs are collected, which can be described as follows [28,15]:

- Video Segment Latency: the delay of the transmission between video segments on a video transmission throughout the network;
- Service Reliability: the percentage of time that the service is provided to the client within the desired parameters;
- Bandwidth: the number of bits per unit of time relative to the video transmission streams;
- Time, Spatial, and Quality Resolutions: the video fragments are received at the application level.

The indicators can provide an assessment from the physical layer to the network layer (performance indicators) and from the transport layer to the application layer (quality indicators) of the network under scenarios of video and audio transmissions in the vehicular environment.

3.2. Gathered metrics for indicators

To monitor 5G and next-generation mobile network traffic, we must focus on metrics that will reflect the indicators stated in the subsection abovementioned.

The performance analysis will be directly related to the network system and infrastructure below. This assessment should provide an interpretation of the performance of the technologies in use by the network architecture, quantifying such parameters under a set of expected values (for the 5G standards). Here, such metrics can be retrieved:

- Packet Delay: time between the occurrence of two corresponding packet reference events;
- Packet Jitter: variations in packet delay;
- Packet Loss Ratio: ratio of total packet outcomes to total transmitted packets;
- Transmitted and Received Bytes and Rate: number and rate of good transmitted and received bytes.

An analysis of the metrics provided by the audio and video stream, at a layer above the network performance data gathering, will be directly related to the perceived quality and factual quality. These metrics will also be related to the underlying network's performance, providing a better understanding of the overall network performance and multimedia content visualization experience. For this matter, the quality metrics that will be considered for this assessment are as follows:

- Audio and Video Delay: end-to-end one-way delay in audio and video;
- Audio and Video Download: time from the first byte being received in audio and video to the last byte in the transmitted segment;
- Audio and Video Ratio: ratio of the video segment playback time to total download time over the last N segments;
- Audio and Video Buffer Length: time of audio and video already buffered at a given time;
- Audio and Video Average Throughput: audio and video average throughput in the end-to-end one-way transmission;
- Audio and Video Bitrate: audio and video bitrate as defined by the stream information;
- Audio and Video Dropped Frames: end-to-end audio and video frames dropped as a consequence of packet losses;
- Video Segment Duration: video segment duration as retrieved by the stream information.

To measure its success, the measurement of the visualization experience by a user is no trivial task. The experience may be considered an overall abstract aspect; therefore, several concepts must be discussed to justify the assessment. These concepts are related to user engagement, which will vary based on the performance and quality of the service provided (and even the user itself). Therefore, to evaluate the experience, some key aspects need to be taken into account, in order of priority concluded by the works in [29–31]:

1. Buffering ratio (percentage of time spent in buffering): as expected, the number of times a video stops due to an empty buffer and the duration it takes to rebuffer are directly linked to user engagement levels;
2. Video quality (average bitrate): nowadays a user expects a good quality for the visualization of multimedia content, and a high fluctuation of video quality during a video stream makes users lose interest in watching the respective video;
3. Joining times (time for the video to start playing): beyond 2 seconds, users start to abandon the video; the total length of the video also affects the waiting time the users are willing to wait for the video to start, as well as the device in which the users are watching the content.

With this in mind, the following metrics will be considered for this assessment on experience:

- Video Resolution: spatial resolution of the transmitted video;
- Client Resolution: spatial resolution of the played video;
- Video Frame Rate: frame rate used in the video encoder;
- Video Adaptability: average selected video bit rate per segment in a stream over the minimum of either the average throughput available or the maximum available representation;
- Video Re-buffering: characterization and quantification of re-buffering events within a streaming session;
- Video Visualization Time: current and total time of the current streaming session.

Some of these metrics are gathered already as an estimated value considering variables in a probing system, as they are contextualized within the communication layers below. Therefore, in a composed manner, some metrics arise, such as the video adaptability, the video adaptation frequency, video adaptation amplitude, the video re-buffering amplitude, and the video re-buffering frequency [32,33].

The video adaptability metric (A) is an average of the chosen video bit rate (R_i) per segment (within K segments) over the minimum of either the average throughput available during the current segment σ or the maximum available representation R_N, given by

$$A = \frac{1}{K}\sum_{i=1}^{K}\frac{R_i}{\min(R_N, \sigma_i)}. \quad (1)$$

The video adaptation frequency indicator (AF) is the number of representation switches over the K total number of segments and is given by

$$AF = \frac{\sum_{i=1}^{K-1}\left(1-\delta_{R,R_{i+1}}\right)}{K}, \quad (2)$$

where δ is the Kronecker delta.

On the other hand, the video adaptation amplitude metric (AA) expresses the normalized average distance, in terms of bit rate, between the representation levels and is given by

$$AA = \frac{1}{K \cdot AF} \frac{\sum_{i=1}^{K-1} \left|1 - \delta_{R,R_{i+1}}\right|}{R_{\max}}, \tag{3}$$

where $R_{\max}$ is the maximum available representation.

Regarding re-buffering events, the video re-buffering duration indicator (RD) means the total duration of re-buffering events in a stream over the length of the played-out video L and is given by

$$RD = \frac{\sum_{i=\omega+1}^{K} \beta_i \cdot \left(t_i^{\text{end}} - t_i^{\text{start}}\right)}{L}. \tag{4}$$

The RD reconsiders K segments, in which $\beta_i = 1$ if a re-buffering event has occurred during the download of segment i, and $\beta_i = 0$ otherwise. The values of t_i^{end} and t_i^{start} are the time of the end and the start of the re-buffering event. They occur during the download of the segment i, and ω means the re-buffering threshold (the number of segments that need to be downloaded in the buffer before play-out can resume after a stall event).

In terms of the video re-buffering frequency indicator (RF), it represents the number of re-buffering events that occur in a stream over the number of segments K and is given by

$$RF = \frac{\sum_{i=\omega+1}^{K} \beta_i}{K}. \tag{5}$$

4. Probe architecture and implementation

The KPIs and KQIs were defined for the scope of this work, taking into account the vehicular environment for multimedia communication. To produce meaningful information, a probe should be placed within the communication paths to gather the metrics specified by each KPI and KQI. Such a probing mechanism, as it was designed, is considered to control or give hints to others to take control over the available video streams in a server. With the primary goal of retrieving metrics related to performance, quality, and experience, a complete evaluation of the network and the respective multimedia session is performed under the scope of the vehicular environment in a 5G context.

4.1. Architecture

In Fig. 2 one can identify the presence of a server-client architecture in which a video stream is transmitted from the server to the client requesting it. Within the communication path, a customer premises equipment (CPE) which grants the client a connection to the outside network (such as the Internet) accommodates this probing mechanism as cooperation of three modules.

As mentioned, the CPE is an intermediate node to our system, placed between the server and client of a video transmission, in which our probing mechanism resides. This mechanism is then comprised of three main modules that take care of the metrics retrieval in different sets of communication layers. First, a performance module is responsible for capturing data from the physical to the network layer. This is done by assessing its connection with the provided access network and from the external network to which it is also connected, both in terms of the physical medium and packet-level metrics.

Secondly, a quality module allows the probe to get information extracted from transport layers of communication (layer 4), whose goals are to estimate and retrieve metrics provided by the audio and video streams.

Finally, a module of experience allows the probe to infer and estimate metrics directly related to video characteristics, as described in the previous subsection, of video adaptability, adaptation, and re-buffering event characterization.

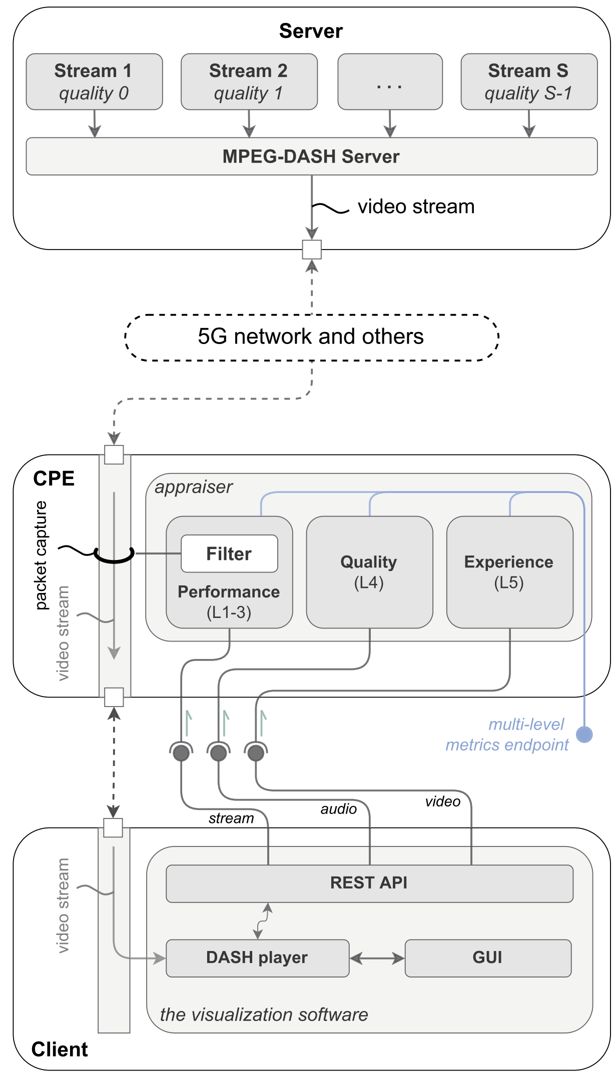

Fig. 2. Global architecture of the probing approach.

Inside the performance module, several logical layers are displaced to categorically extract and differentiate metrics from different sources and procedures. As previously mentioned, to get information from a physical to a network layer, this module should be able to retrieve information directly: from the network interface card (NIC) (or low-level requests from its inner network modem device, such as the execution of AT commands); from the system's kernel where the NIC is installed; from estimating metrics on packets from the CPE to its gateway to the external network; and packets from the CPE to the video server. These procedures can be made with the help of a packet capture device, represented in Fig. 2 by the filter submodule.

4.2. Implementation choices and considerations

To deploy the designed probing approach, some considerations and choices were made. To implement the designed system as depicted in Fig. 2, both server and client must be previously chosen or created to accommodate and perform video transmissions.

After analyzing the state-of-the-art video streaming transport methods and technologies, MPEG-DASH streams were chosen to serve as the basis of the probe development [34,35]. They are codec-agnostic and will allow considering a video streaming server and client to adaptively choose video stream variations according to the capabilities of the network reception. This choice allows us

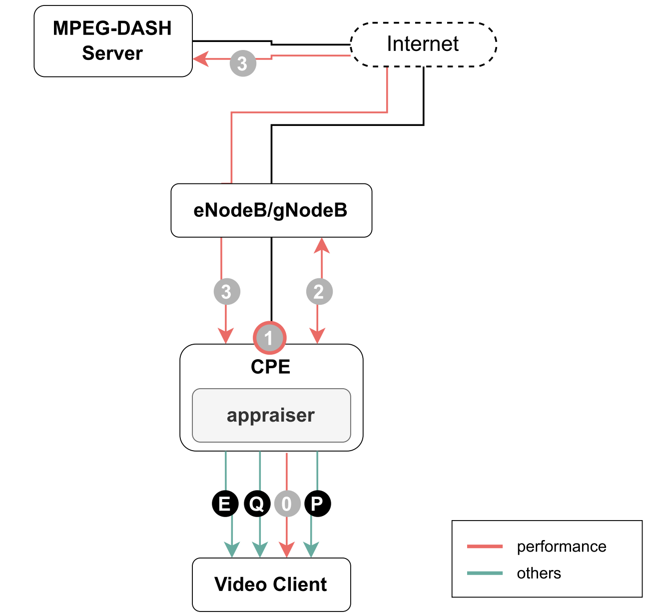

Fig. 3. Metrics gathering locations within the proposed architecture.

to conduct tests on streams with S different variations on spatial, time, and quality resolutions.

On the other hand, since we have chosen to use an MPEG-DASH video server, we need a client to reproduce these contents. This way, our client will consist of an MPEG-DASH with a proper service providing the CPE with a set of metrics related to the video stream being played at a given time.

Relatively to the CPE node, this equipment will be responsible for providing clients as a gateway to an external network accessed via 4G or 5G.

4.3. Gathered metrics

As previously defined, the CPE is the main metrics aggregator in this architecture. To aggregate the maximum meaningful data possible, metrics are to be gathered both in the client direction (to retrieve the current status of both visualization and reception of video data), and in the server direction (to retrieve the current status of the network connection, locally, to and from the gNodeB, and with the video server). Fig. 3 illustrates the locations where metrics are gathered, as aggregated in the CPE device.

Starting with the metrics gathered from the client, with the help of a developed software that provides the client with a proper video player capable of reproducing MPEG-DASH content, the listed metrics concerning the described experience and quality modules are retrieved and aggregated in the CPE. The client, whose MPEG-DASH was made based on the MPEG-DASH *dash.js* reference client,[1] publishes a proper API with two endpoints for each metrics module, as depicted in Fig. 3 by the marks Ⓔ and Ⓠ.

On the other hand, considering the same figure, the performance module Ⓟ performs network metrics captures at different levels. At a first level, it captures network interface-related metrics, as marked by the number ①; at a second level (marked as ②), it captures metrics for a given and present network interface related to the communication with the gateway. At a third level, it captures metrics related to the communication with the respective streaming video server, as marked by ③. Network-wise, a set

[1] https://reference.dashif.org/dash.js.

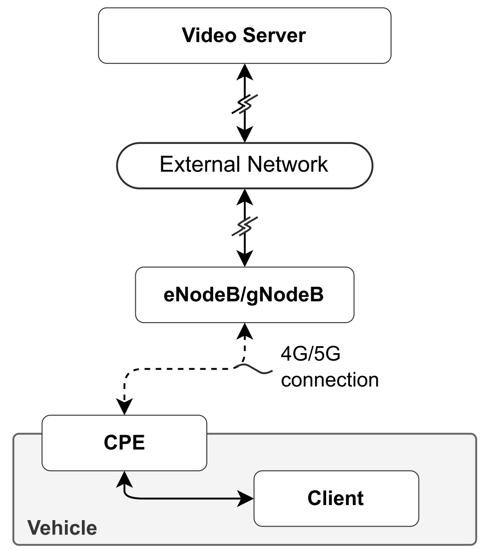

Fig. 4. Diagram of V2I testing scenario.

of metrics is retrieved, such as delay and jitter to the gateway or the video server in use by the stream.

Downwards the physical layer, a final part of the performance module Ⓟ is comprised of a last endpoint whose responsibility is to expose the radio metrics to help correlate the video KPIs with the state of the cellular service. The most important KPIs to measure the quality of the connection are then obtained in this endpoint, such as the received signal strength indicator (RSSI), reference signal received quality (RSRQ), reference signal received power (RSRP), and signal-to-interference-noise ratio (SINR) (for both 4G and 5G connections), and it also allows the CPE to receive geographical coordinates on the client state. This data collecting endpoint is marked in Fig. 3 as ⓪.

5. Test scenarios and services

The probing approach retrieves multi-layer key performance indicators (KPIs) during video transmissions in the context of a connection to a 5G (and 4G) network. For this purpose, two scenarios were designed to estimate metrics from a video transmission session within a 5G vehicular context. In this section, we describe both scenarios, ending with the exposition of results, followed by a discussion.

5.1. Testing scenarios

In the first scenario, we designed a vehicle-to-infrastructure (V2I) topology where a user is within a vehicle and requests a video being transmitted (or is accessible) via a remote video server, which can be external to the 5G (and 4G) network context. Thus, a video server resides outside the network, such as in a remote datacenter; users are in vehicles and use the connection granted by the network to access the content through a proper gateway providing such a connection.

As depicted in Fig. 4 and to support such a scenario, a 5G customer premises equipment (CPE) is used inside the vehicles to allow clients to connect to a 5G (and 4G) network in order to access the requested video content. This CPE is designed to run an instance of the network and video QoE monitoring as proposed in Fig. 3.

The monitoring component that runs within the CPE instance is an aggregator of multi-layered KPIs. These metrics cover all the communication protocol layers of a computing system, from a physical layer (relative to the connection medium factors) to an

Table 1
Test batches configurations of all performed tests in V2I, regarding to cellular standard and saturation level of the radio access technology (the saturation level is provided with IPerf, in Mbps).

Access Technology	level 1	level 2	level 3
4G	0 Mbps	10 Mbps	20 Mbps
5G	0 Mbps	125 Mbps	250 Mbps

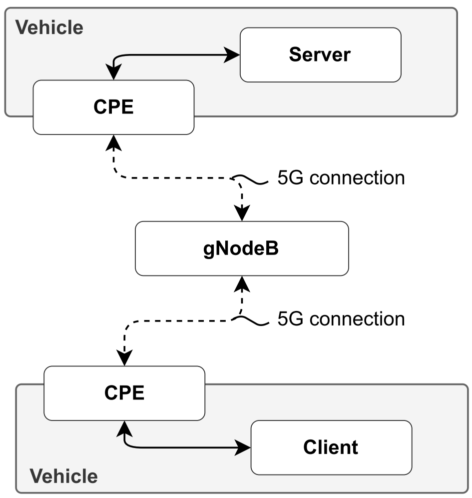

Fig. 5. Diagram of V2V testing scenario.

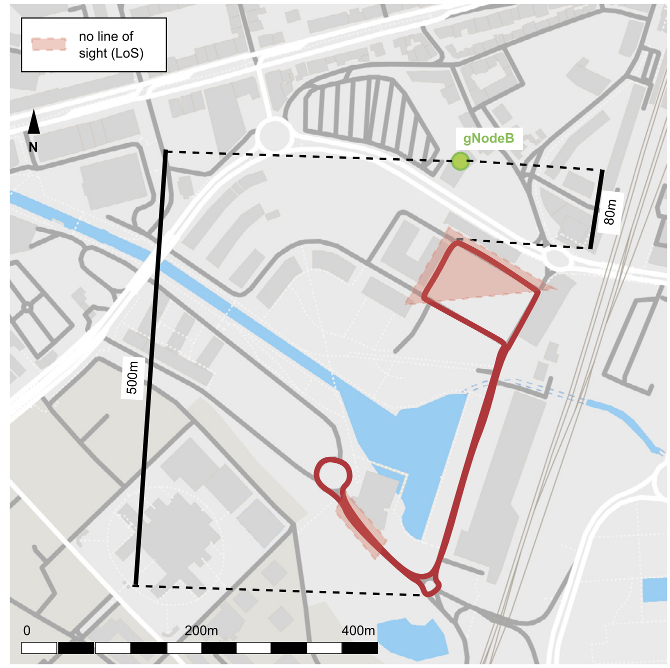

Fig. 6. Test circuit at Fonte Nova Pier, Aveiro, Portugal, within the proximity of a 5G gNodeB.

application layer (relative to video aspects, inherent to the user's experience that demands the video content to be watched).

In this first scenario, tests were designed to allow clients on a vehicle to connect to a video instance outside the network to which they belong or have a direct connection. In order to change the conditions of the connection with which the users are requesting video content, saturation must be produced with different bandwidth levels by using a network profiler tool such as IPerf.[2] Within this scenario, and to further compare the results with LTE/4G (considering it as a baseline), we designed tests to be executed as described in Table 1.

In a second scenario, the video server is moved from an external context to the 5G network to an internal and almost direct connection from the CPE device. The video server instance is placed in a second vehicle, where clients on a vehicle, through the use of the CPE (working as a gateway to the 5G network), connect and demand video content from a video server running on a different vehicle, connected via a second CPE. The video is sent from a video camera that shows information from the road and surroundings directly to other rear vehicles. Although we name this scenario as vehicle-to-vehicle (V2V), the present connection between the pair server/client, video-wise, is not performed directly. Instead, the connection is made by passing through the gNodeB, providing 5G links to both CPEs. A representation of such a scenario can be found in Fig. 5.

5.2. Infrastructure and equipment

To perform the tests in a real scenario and with a real 5G testbed, we created a circuit in the city of Aveiro, Portugal, that takes advantage of the already deployed 5G non-standalone (NSA) infrastructure. Choosing the Fonte Nova Pier site in Aveiro, as depicted in Fig. 6, we took advantage of a 5G link-capable area with a maximum distance to the gNodeB of 500 meters, and with more than half of the circuit granting a line-of-sight (LoS) from the CPE's antennas to the base station.

This circuit is to be used in both V2I and V2V testing scenarios, and was designed to keep a record of speeds in common with the normal traffic conditions of the chosen public space, varying between 30 km/h and 50 km/h. Running our two vehicles under test in opposite directions in the designated circuit, their distances differ between 0 m and 420 m. With 25% of the circuit lacking line-of-sight with the gNodeB in two sections as depicted in Fig. 6, while the two vehicles are running, the circuit confers a maximum of 35% of the route in which at least one of the vehicles does not have line-of-sight, and a maximum of 21% where both simultaneously does not reach line-of-sight.

The cellular network used was a test network implemented in the city of Aveiro by the internet service provider Altice MEO[3] within the scope of the Aveiro STEAM City project[4] resulting from the Urban Innovative Actions (UIA) Community Program, where the goal is to promote the adoption of 5G and Internet-of-Things (IoT) infrastructures and technologies in the city.

In terms of technical characteristics, this network characterizes by being an NSA network in the band 78, occupying 100 MHz of bandwidth between 3.6 GHz and 3.7 GHz for the 5G connection, and having a 4G channel at 2.6 GHz. In addition to the base station identified in Fig. 6, there are also two others in the city, as depicted in Fig. 7. Although this is a test network and a specific and pre-known SIM card is required, the infrastructure is shared with MEO's commercial network; as such, whenever there is no connectivity from one of these three base stations, the connection is guaranteed by the commercial infrastructure.

Regarding the used hardware and software, in Table 2 the specifications for the equipment used as CPEs are shown in detail, briefly being a compact x86 UNIX-based platform.

For the 5G connectivity, there are two modems based on the Qualcomm's chipsets being the Quectel RM500Q-GL and the SIM-

[2] https://iperf.fr.

[3] https://www.meo.pt.

[4] https://www.uia-initiative.eu/en/uia-cities/aveiro.

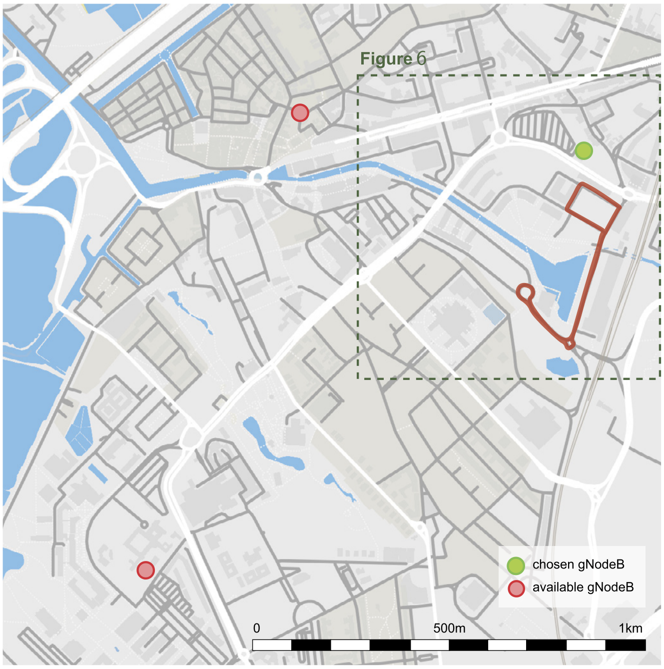

Fig. 7. Location of the three gNodeB in Aveiro, Portugal.

Table 2
CPE hardware information (PcEngines APU).

Property	Description
CPU	AMD Embedded G series GX-412TC, 1 GHz, 64-bit, 2 MB L2 cache
DRAM	2 to 4 GB DDR3-1333 MHz
Storage	SD card, external USB or m-SATA SSD
Power	12V DC, from 6 W to 12 W, center positive 2.5 mm jack
Connectivity	3 gigabit Ethernet channels (Intel i211AT or i210AT)
I/O	DB9 serial port, 2 USB 3.0 external and 2.0 internal
Expansion	2 miniPCI express (one with SIM socket), LPC bus, GPIO header, I2C bus, COM2 (3.3V RXD/TXD)
Board size	152.4 × 152.4 mm

Table 3
Quectel and SIMCOM 5G used modem specifications.

Property	Quectel RM500Q-GL	SIMCOM SIM8200G
5G Data Rates *(up to)*		
Downlink	2.5 Gbps	5 Gbps
Uplink	650 Mbps	450 Mbps
4G Data Rates *(up to)*		
Downlink	1 Gbps	2.4 Gbps
Uplink	200 Mbps	200 Mbps
Interface	USB/PCIe	USB/PCIe
Dimensions (mm)	30.0 × 52.0 × 2.3	30.0 × 52.0 × 2.3
Form factor	M.2 3052	M.2 3052

COM SIM8200G. The use of one of them depends on their availability during the execution of our tests, as well as on the firmware maturity of each manufacturer. Table 3 shows the specifications for both models.

5.3. Multimedia service

At the video client side, a proper video client is being used, able to connect and adequately decode and rearrange frames of an MPEG-DASH video stream, as our video server is streaming it. Consequently, this client can switch from several levels of quality regarding some QoE metrics, such as the video resolution, video bitrate, or consistency of the buffer length being filled throughout the time.

Table 4
Set of video qualities for the chosen video stream.

Level	Resolution (width × height)	Bitrate (Kbps)	MOS
1	426 × 240	100	2
2	426 × 240	300	2
3	426 × 240	500	2
4	426 × 240	700	2
5	640 × 360	400	2
6	640 × 360	600	2
7	640 × 360	800	2
8	640 × 360	1000	2
9	854 × 480	500	2
10	854 × 480	800	2
11	854 × 480	1100	2
12	854 × 480	1400	2
13	854 × 480	1700	2
14	854 × 480	2000	2
15	1280 × 720	1500	2
16	1280 × 720	2000	2
17	1280 × 720	2500	3
18	1280 × 720	3000	3
19	1280 × 720	3500	3
20	1280 × 720	4000	3
21	1920 × 1080	3000	3
22	1920 × 1080	4000	3
23	1920 × 1080	5000	3
24	1920 × 1080	6000	3
25	2560 × 1440	6000	3
26	2560 × 1440	8000	4
27	2560 × 1440	10000	4
28	2560 × 1440	12000	4
29	2560 × 1440	13000	4
30	3840 × 2160	13000	4
31	3840 × 2160	15000	4
32	3840 × 2160	20000	4
33	3840 × 2160	25000	4
34	3840 × 2160	30000	4
35	3840 × 2160	34000	4

Such a video stream is constantly transmitting a one-minute length video entitled “The Daily Dweebs”, a synthesized animated video we chose to be our testing video. This choice was made due to many video quality levels available for streaming and different bitrates and video resolutions, as shown in Table 4. In this same table, one can also see a MOS value which corresponds to an assessed record using a video QoE scoring model by Salvador et al. [36], in other to easily relate a subjective scaled value regarding quality of experience. In this model, the mean opinion score is obtained relatively to variations of the video bitrate, screen size and video size ratios, frames per second, and the number of buffer stalls.

6. Results and discussion

This section depicts and discusses the results on both V2I and V2V scenarios.

6.1. Test results on V2I scenario

In the first scenario we have executed batches of tests in both 4G and 5G access technologies, within a scenario of vehicle-to-infrastructure, with the configurations shown in Table 1.

We first analyze a comparison between technologies, where we show a summary of a set of 5 tests (where the lines represent the average value of the test results, and the background corresponds to the results' standard deviation) done under both 4G and 5G connections (in motion), with a similar mobility function. These results are depicted in Fig. 8 and cover different levels of the OSI communication stack model: in a physical layer, showcasing val-

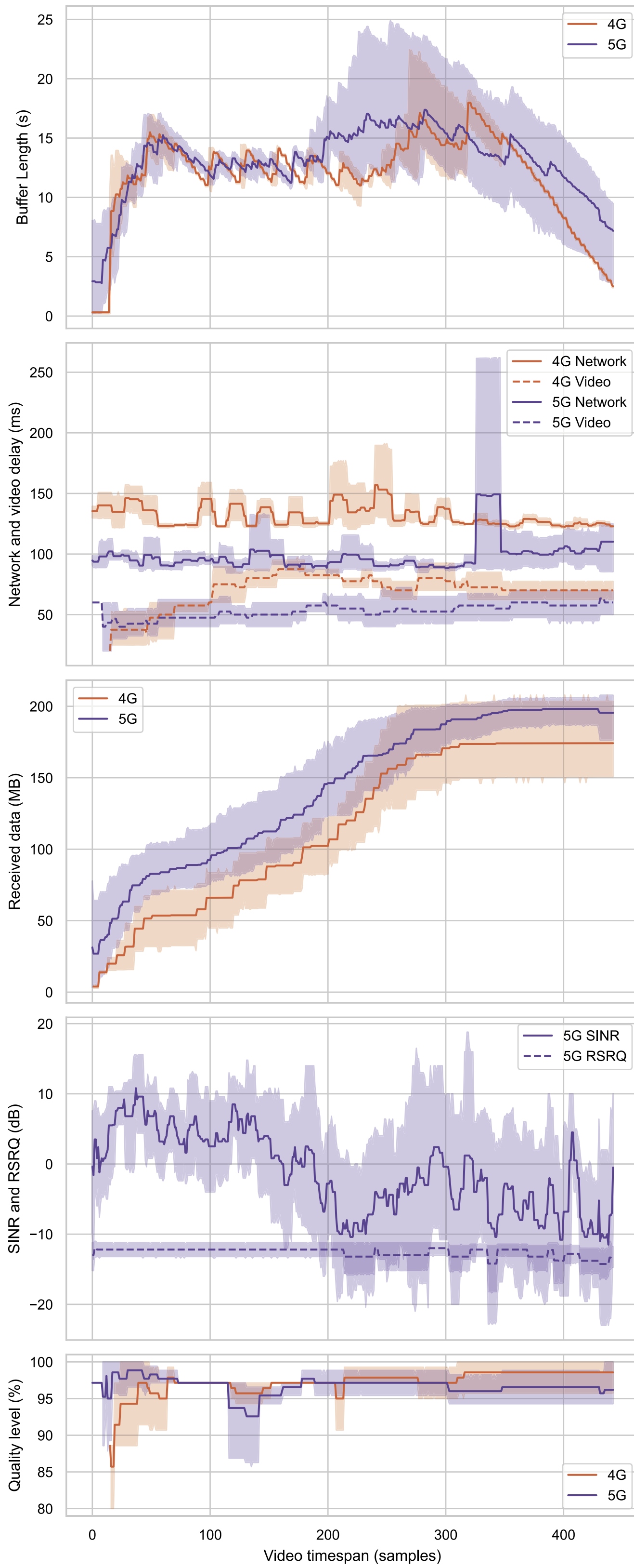

Fig. 8. Tests, in mobility, with LTE and 5G, without saturation.

ues of SINR and RSRQ; in a network level, covering the number of megabytes received in a receiving network interface card and the network delay; in an application level, where details on the video delay and buffer length are considered. Moreover, at the end of this figure, sharing the same *x*-axis which relates to the timespan of the 1-minute length video (from the beginning to the end), there is a plot regarding the quality level given as a percentage of the current level (from 1 to 35, as described in Table 4), in respect to the maximum level of 35, which can be translated onto a model-based MOS assessed value, as described in Table 4.

In these tests, the received data corresponds to all data frames, represented in megabytes (MB), gathered in the network interface card from which a connection from the gNodeB is granted. The reception rate is consistent until a moment when no more frames are being received. Still, one can verify that the received data in 4G is lower than in 5G.

Relating with other metrics, one can then bridge these results to the buffer length. This metric relates to a data structure that is consumed at a different rate as it is filled. This happens since every inserted frame does not have to be, in any way, equal to the length of other frames already handled. One can relate the received data with the buffer length since the buffer length takes a median value of approximately 15 seconds, receiving fewer frames in the middle of the video timespan due to the amount of encoded and transmitted bytes being higher in some video segments. Considering the chosen video, and due to a more significant amount of motion to be encoded in the region right after half of the video timespan, it is probable that the client has slightly more difficulty loading more data than what is being consumed.

Taking advantage of a lower quality level, meaning that the frame lengths are lower and easier to download, the buffer length gets to a maximum of approximately 25 seconds. As soon as the received data related to the video gets a constant rate, the buffer length starts a period of consumption-only. This happens since no more frames are to be received unless new data is required after the MPEG-DASH triggered a new video quality level to be received.

Above the network level, we can also observe the behavior of the video delay versus the network delay. As for the video delay, this is the average time (in milliseconds) from the request of a segment to the reception of its first byte over four requested segments. Since we cannot have a video without a network connection, we cannot have a video delay with a higher order of magnitude than the network delay, which we can verify by analyzing the second plot in Fig. 8, in both cases of 4G and 5G. While in all cases the network delay is upper bounding the video delay, there are some cases where the network delay has peak values which take no consequence (or residual consequences) in terms of video delay (one instance of this can be stated in between samples 300 and 350, regarding the 5G transmission).

On the other hand, regarding the transition from the network to the communication layers below, we can also verify that there is a relation between the SINR and the received data: as SINR values get mostly below 0 (in the second half of the video), the video quality level oscillates more regularly throughout the visualization time, also lowering the slope of the received data in time, and producing a higher network delay. At the end of these captured results, 4G measurements show a more regular presence of higher quality levels than 5G's results, which can be justified by the fact that 4G can save more segments into buffer while on a better quality than 5G. This is due to the dynamic adaptive bitrate algorithm of MPEG-DASH, which switches smoothly between a buffer occupancy strategy and the assessment of throughput measurements [37].

Now, we insert parallel traffic to the video transmission in the video-server-to-client direction with the help of IPerf: 10 Mbps in the 4G connection, and 125 Mbps in the 5G connection, as mentioned in Table 1. The results are depicted in Fig. 9. The same conclusions can be taken concerning 4G: the increase of the received data is accompanied by the buffer length in the ranges where the

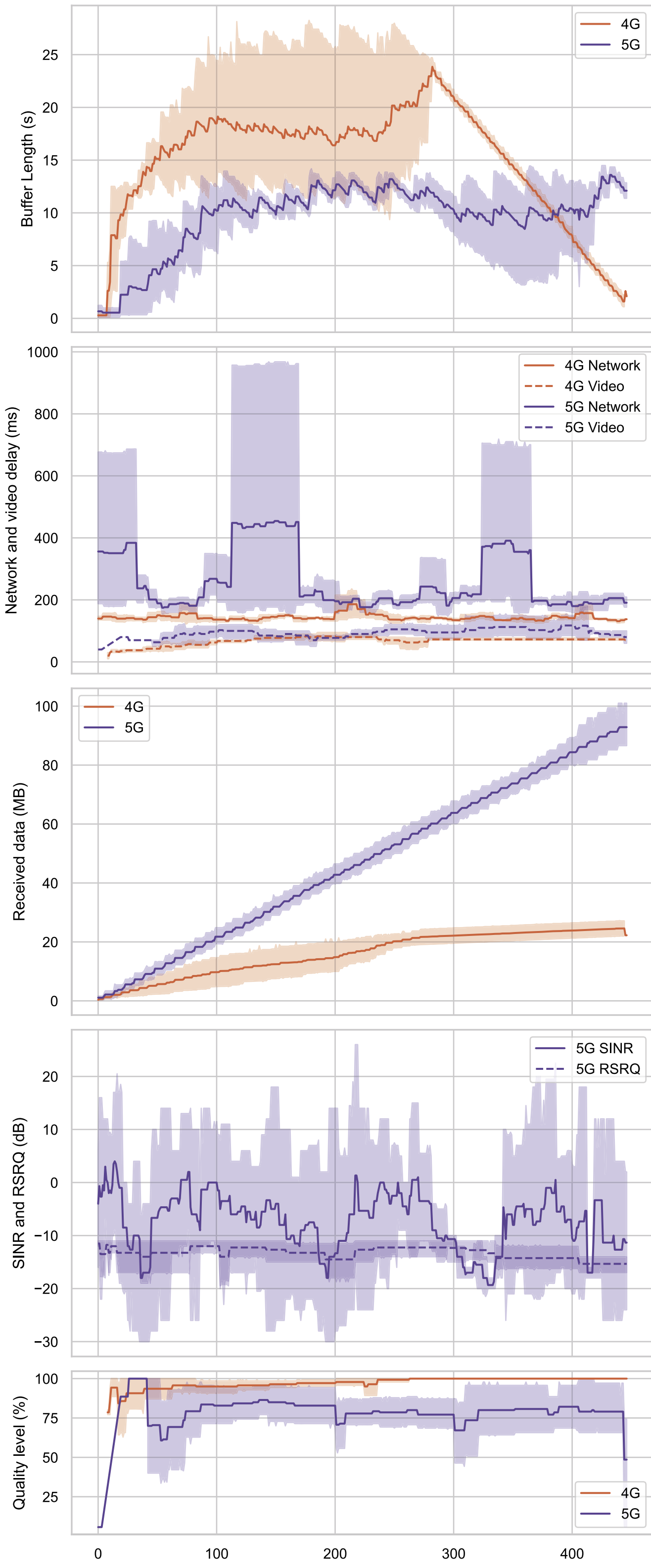

Fig. 9. Tests, in mobility, with LTE and 5G, with a saturation of 10 Mbps (in 4G) and 125 Mbps (in 5G).

amount of data in the transmission is, inherently, more consistent throughout the video length. Also, regarding network and video delay, the network delay shows up to vary a little without causing further damage to the video delay while upper bounding it.

Now considering the 5G test batches, one can verify that the received data amount does not reach a near-constant rate during the visualization of the video. This fact can be corroborated by the buffer length, which did not achieve a consumption-only period during the video timespan. With this, one can also verify that the buffer length maintains a pattern where a time range in the middle of the video length has more difficulty growing, which is why the buffer cannot end empty since there is a larger delay associated with the video process. As the quality level plot shows, there is more loaded buffer data from several quality levels, as requested in different instants.

Moreover, in these examples, one can also observe that the video visualization was severely disturbed by the physical conditions, as shown in the decrease in SINR in sampling ranges of 40-50, 180-200, and 280-350. Here, the SINR dropped below −10 dB, also decreasing the RSRQ, and propagating issues to the network delay that grew higher, augmenting the video delay and causing the video quality level to drop substantially (below the 75%).

Regarding the next step in saturation levels, as shown in Fig. 10, we attempted to gather metrics with parallel traffic being generated with a bandwidth of 20 Mbps in 4G and 250 Mbps in 5G. In these tests, first in the 4G set, we can observe that the generated traffic did not quite interfere with the video transmission, as the video quality, despite some variation dropping to a maximum of approximately 20%, mainly remained equal, and at a high level. Regarding the received data, we can observe that compared with the experiments before, the slope is higher in this example, leading to a completely different fill of the buffer length, where the most frames could be gathered right in the first 20 seconds of visualization. Although this may look odd, this can happen with this growth factor since, with a lower video quality level, frames do have smaller lengths and bitrates (as confirmed by the information in Table 4), which will not induce the former shapes to the buffer length plot.

In terms of 5G, a different perspective was gathered, in which the generated bandwidth was higher enough to cause issues transmission- and visualization-wise. Despite the received data looking all similar in slope to the experiments before, and as shown by the 4G case analysis, the slope is higher due to video frames being smaller in length and with lower bitrates. Moreover, these results also happen due to the MPEG-DASH mechanism requesting multiple video quality levels throughout a streaming session, which is a consequence of a higher network delay. These values, probably generated by captured instabilities by the physical metrics such as the RSRQ and SINR, lead to a vast majority of time suffering issues in each experiment. The buffer length stays constant at an average time, meaning that the rate at which the buffer data was consumed was similar to the reception rate. Taking a cross-layer perspective, one can again verify that the SINR impacts more in the quality level when compared with the RSRQ. For instance, in timestamps between 200 and 300 of the video timespan, the video quality level significantly dropped as soon as the SINR dropped below the −10 dB level.

Moreover, one can also verify that, even with a lower quality level as requested by the MPEG-DASH stream client, these results are achieved due to very high oscillations in the network delay and, consequently, in the video delay as well. Despite this occurrence, as a buffering is being made with smaller video segments, this does not impact the video stalling, which is a reason not to have any rebuffering events during the video timespan.

Focusing on metrics regarding the video transmission adaptation, which allows inferring parameters or limitations for QoE, in Fig. 11 one can observe two plots over the quality level: one for adaptability and the other for video adaptation amplitude. These plots aim to summarize all experiments with 5G tests, differing its

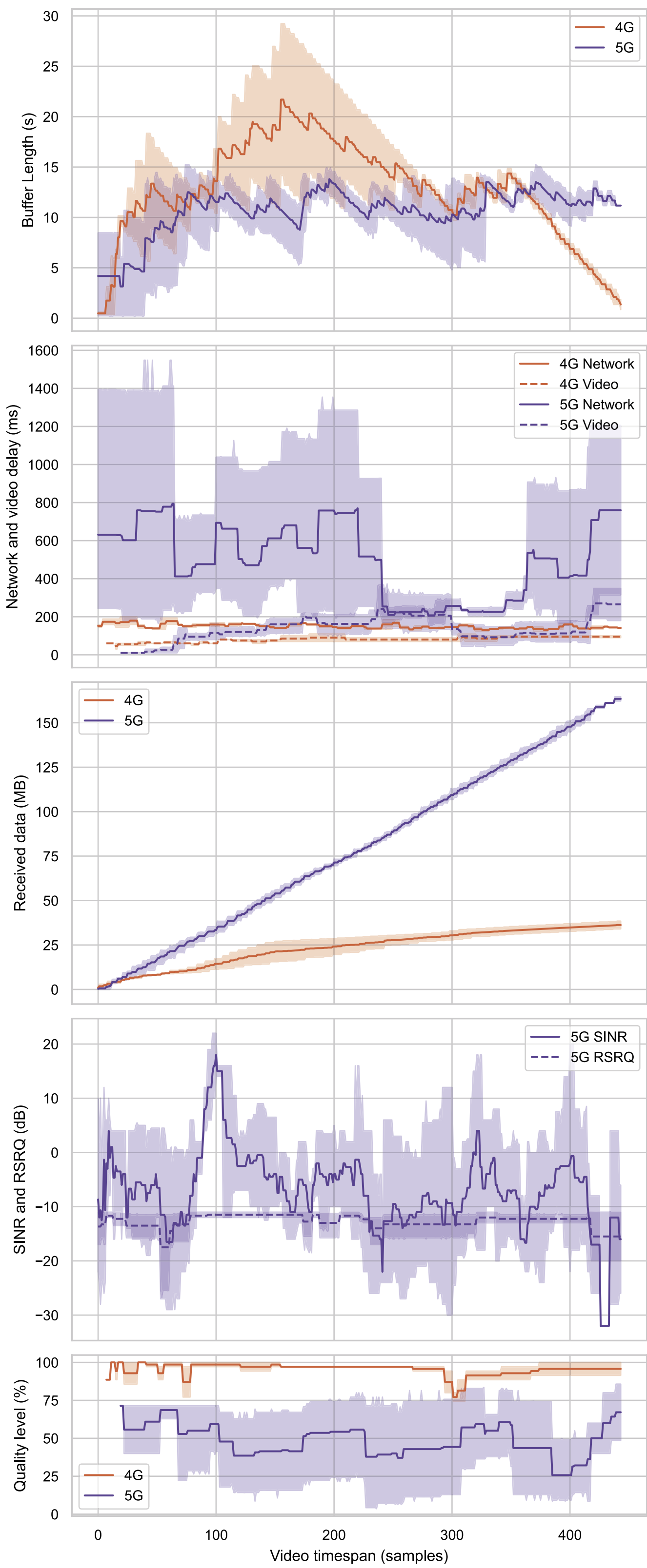

Fig. 10. Tests, in mobility, with LTE and 5G, with a saturation of 20 Mbps (in 4G) and 250 Mbps (in 5G).

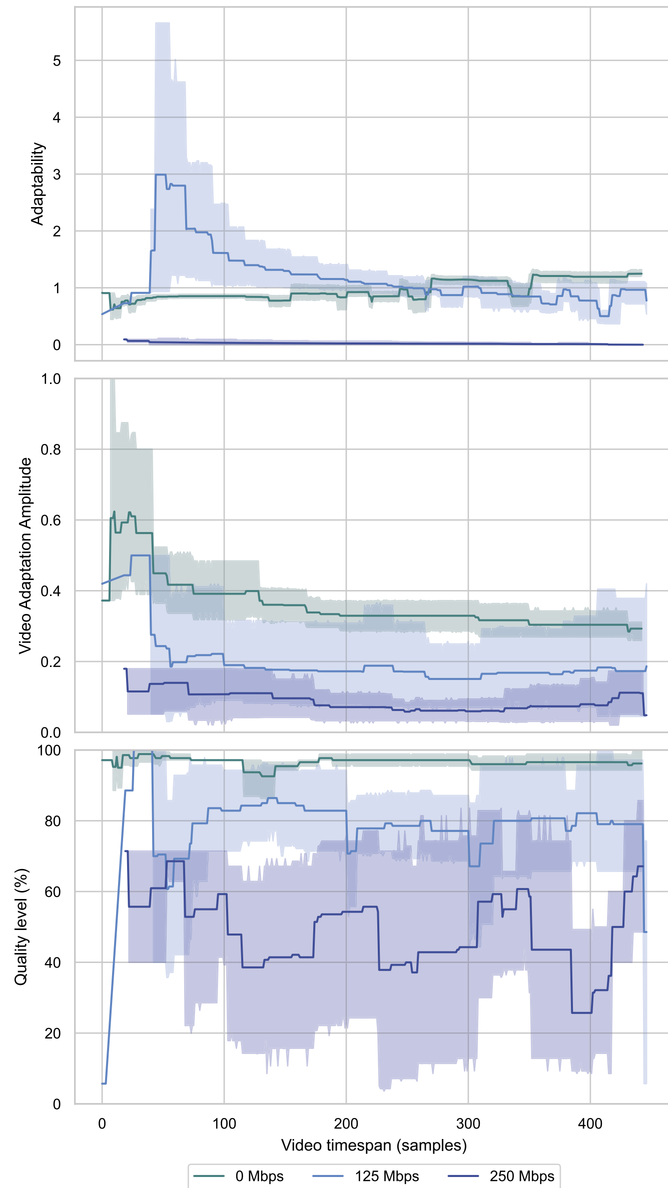

Fig. 11. Tests, in mobility, with 5G and regarding experience metrics of adaptability and video adaptation amplitude, per saturation levels.

behavior in terms of the set of saturation levels introduced in the transmission by the IPerf tool.

The first conclusion we can get from the adaptability and video adaptation amplitude is that, as expected, both values are better regarding the non-saturated environment, followed by when the saturation is intermediate and then maximum. As represented in teal color, the adaptability level when there is no active saturation maintains itself with an increasing monotony around 1, meaning that the video transmission is adapting itself positively within the number of transitioned representation levels (which in this case is as low as 3 levels).

In fact, this might be difficult to understand when one compares this conclusion with the line on the saturation of 125 Mbps, as adaptability levels grow high as 3 at the beginning of the video timespan. These results are misleading since there were problems with the buffering right at the beginning of the video, as we can observe in Fig. 9. This led to the video quality level suddenly loading at a high value, which allowed the MPEG-DASH algorithm of choice [of video quality] to assess the transmission capabilities and then reduce the value to a more appropriate one. With these variations, the adaptability increased, converging then to a more significant value, which can be seen below the non-saturated line's adaptability values.

In contrast, in the case of 250 Mbps of saturation and as the quality level changed in a wide range between 30% to 70%, such occurrence is evidenced by the low values of adaptability (near 0). This occurrence means that the video could not adapt to a point its visualization was put at risk of not being able to pass information. The same is shown by the video adaptation amplitude, as its normalized average distance between representations allows us to conclude that, despite the video quality constantly changing, the representations being chosen grant more minor variations in bitrate, as shown in Table 4. The results in these experiments have shifted between levels of 10 to 24, matching differences in bitrate from 800 Kbps to 6000 Kbps. At the same time, the saturation of 125 got variations between 6000 Kbps and 13000 Kbps, and the non-saturated got between 20000 Kbps and 34000 Kbps.

6.2. Test results on V2V scenario

Regarding scenario 2, of V2V, only tests within the context of 5G were executed, where two vehicles were moving throughout the designed testing circuit presented in Fig. 6. Tests in 4G were discarded from this stage since preliminary tests with 4G in a V2V scenario could not recover from errors during the duration of the tests due to high latencies. Similar to how we performed in the V2I tests, in these batches of sets of 5 runs, V2V tests we also generated parallel traffic with the help of IPerf, given bandwidths of 0 Mbps, 30 Mbps, and 60 Mbps. Such traffic was generated from the video server to the video client, this is, from one vehicle to another, moving independently of each other.

At first glance, when comparing the results of the V2I with the V2V with no saturation in Fig. 12, one can denote that, despite a lower median value for the physical metrics of RSRQ and SINR, the amount of received bytes per time range was more variable in V2V, rather than in V2I. In opposition to what was stated in the results before, for the first time, we do have values of video delay that are showing up to be higher than the network delay in some of the cases. This event can be justified by the fact that the video server has its connection to serve the content supported on a 5G link, which is also subject to issues in the transmission. This way, the delay estimated by the network metrics can be low. However, the frames allowing the visualization may be higher, given some issues occurring on the video-server-to-gNodeB connection (the probe evaluation considers the video-client-to-gNodeB side).

The lines representing the intermediate level of saturation (of 30 Mbps) infer that more data has been downloaded since variations between requested levels of quality were different during the buffering of the video. This disregards the amount of data added by IPerf since one can notice a slight inflection point between samples 300 and 350.

Moreover, and still regarding the batch of tests with 30 Mbps of saturation in V2V, we can observe a considerable variation in terms of network delay, which was the culprit of a substantial variation regarding video variables such as the video delay, buffer length, and video quality level. As the link conditions cannot reason these substantial variations regarding network delay to the gNodeB, the answer must reside on the 5G link the video server has with its gNodeB, which might have some difficulties at the time of this execution.

Concerning the last batches of tests, where we performed the video transmissions in 5G V2V with 60 Mbps of parallel traffic, the results are visible also in Fig. 12, colored in dark blue. Starting with the video quality level, one can see that the median value drops in the V2V tests, but on the other hand, the physical KPIs are not significantly different from the ones gathered in the V2I tests. Since the video quality level dropped, the buffer length kept

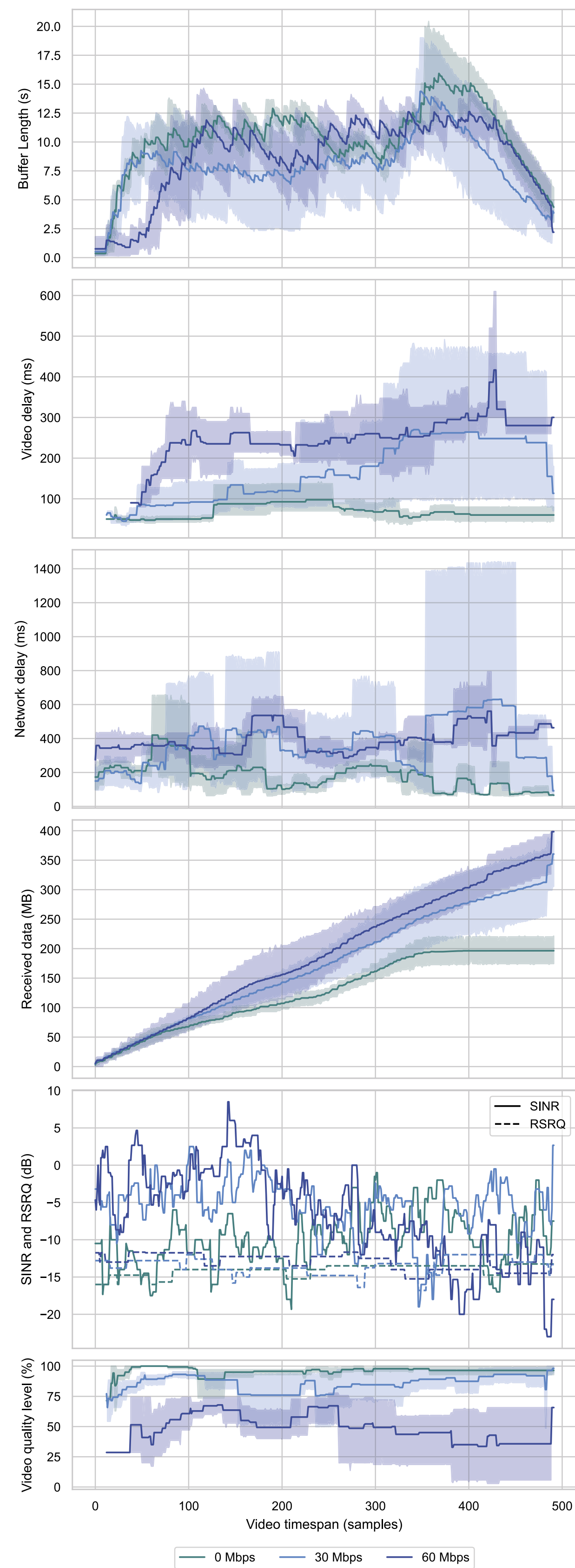

Fig. 12. Complete set of tests of V2V in 5G, with saturations of 0, 30, and 60 Mbps.

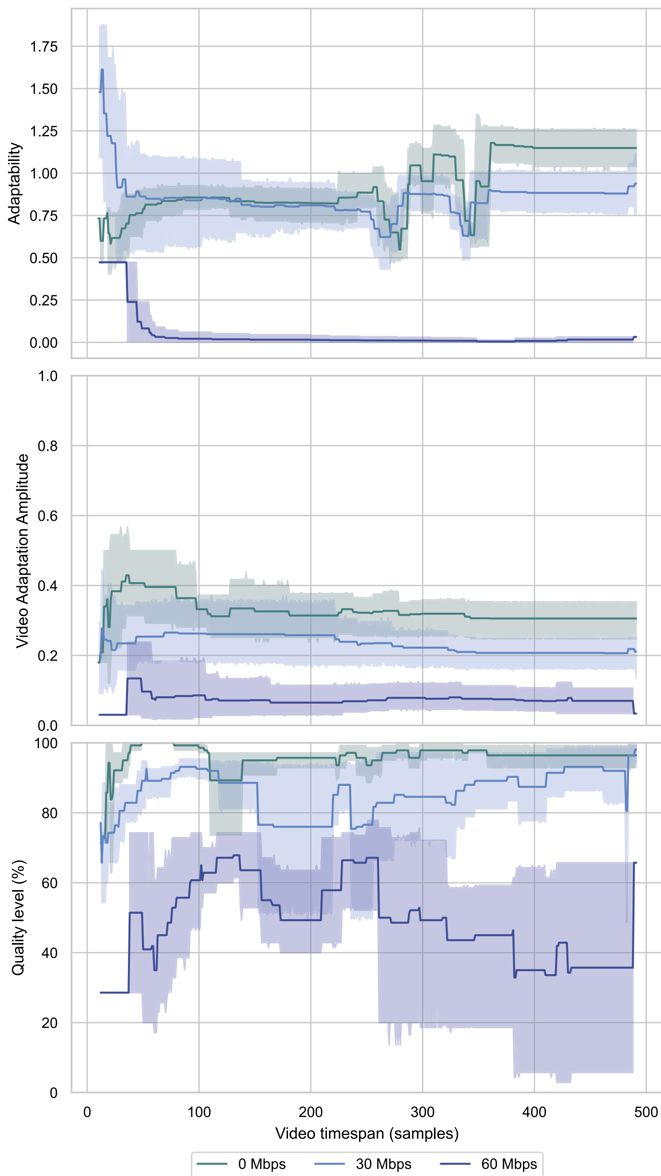

Fig. 13. Tests in V2V regarding experience metrics of adaptability and video adaptation amplitude, per saturation levels.

an expected shape but with frames with smaller lengths and others whose consumption was not fully made due to the variations in the requested quality levels. Once again, the results of V2V also have parameters of video delay higher than the network delay at some time intervals. These properties have conditioned the visualization of the video during the one-minute session, as one can verify by the fact that the buffer length was not fully consumed in all of the performed experiments.

In Fig. 13, we analyze these transmissions from the point of view of our experience module, interpreting the values of both adaptability and video adaptation amplitude. Starting with the numbers in adaptability, one can observe that the data is coherent with the data presented in the V2I scenario: adaptability values for the case where there is no saturation in place are positively approximately 1; for the first level of saturation, the adaptability has an approximate shape, but with a lower value, it is converging to 0.9; and with maximum saturation, as expected by the variations in the quality level, video/network delay, and buffering length, the adaptability is close to 0.

Similarly, regarding the video adaptation amplitude, the trends are again parallel in terms of V2V, with the values of the 30 Mbps getting better due to the variations of video quality levels being higher in bitrate: in V2I they shifted between 6000 Kbps and 13000 Kbps (7000 Kbps of difference), and in V2V they are shifting between 10000 Kbps and 30000 Kbps (20000 Kbps of difference).[5]

6.3. Final remarks

From the V2I to the V2V scenarios, in both analyses, only a subset of the complete set of metrics are exposed, which we considered more relevant to characterize the video streaming sessions in the tested scenarios. As analyzed, the mentioned metrics were sufficient to characterize the video streaming services over vehicular cellular networks. As a subset of the complete set of metrics retrieved, others can be used to fine-tune the characterization of a given system being probed.

During the execution of this probing mechanism, no specific tests were performed to assess the impact of running the developed software within the video streaming sessions. Directly, no interference exists with the network devices since there is no packet mangling throughout the execution of this probe. Mentioning delays to exist, while low-level radio metrics are directly retrieved from the modem, latencies might be relative to processing tasks, produced in the CPE side by the filtering mechanism, where BPF packet captures are done in the ingress interface; and in the client by the REST API publishing the data from the visualization software. As we experimented, and as both CPU and memory usage is low under this probe's execution, extra communication delays can be considered unintelligible.

7. Conclusions and future work

This article proposed a multi-layer probing approach to assess video transmissions over 5G and 4G, combining data from all layers of a communication model. A set of performance and quality indicators was chosen to characterize a video transmission over a 5G network.

The proposed probing approach was tested in both V2I and V2V scenarios. Comparing both network access technology 4G and 5G, in video streaming scenarios, the results have shown that the 5G links show a better overall performance in terms of the video quality of experience, granting lower delays and jitter conditions. This allows video delay to be diminished and segment buffering to be better performed compared to 4G. We also observed that the correlation of multi-layer metrics allowed us to perceive the causes and the manifestation of the induced saturation in the network during the test executions. Mostly visible through the V2V testing scenarios, we observed that non-standalone 5G is susceptible to maintaining the video session up, even when some saturation is in place.

Having gathered the described metrics and performing a video streaming service characterization in cellular vehicular scenarios, one can use such a probing mechanism as input to decision making in components capable of acting preemptively according to the *network* conditions. For example, in a scenario of multiple radio access technologies, a connection manager of an end-user may decide to preemptively select the best network interface according to the metrics collected by the probe.

During our tests, although the chosen video streaming framework of MPEG-DASH performed well for the V2I scenario, such a

[5] A demonstration video of the experiments is accessible via https://youtu.be/hiE22Up0urU.

framework revealed not to be the ideal in a V2V scenario, due to its simpler operations of choosing a different stream representation according only to its buffer usage and throughput.

In the future, this work can be complemented with a feedback mechanism in which the current status of a video transmission can be summarized and delivered back to the CPE or the video server if such a scenario applies. This feedback can lead to changes in the reception and service, which supports the transmissions, allowing them to be enhanced in experience. Moreover, the client is already prepared to collect metrics from the video transmissions and to receive a MOS evaluation from the user, allowing to train a model which can label metric variation signatures as discrete video QoE metrics.

Declaration of competing interest

The authors declare that they have no known competing financial interests or personal relationships that could have appeared to influence the work reported in this paper.

Data availability

No data was used for the research described in the article.

Acknowledgements

This work was supported by the European Regional Development Fund (FEDER), through the Competitiveness and Internationalization Operational Programme (COMPETE 2020) of the Portugal 2020 framework through projects 5G-PERFECTA with Nr. 038190 (POCI-01-0247-FEDER-038190) and IMMINENCE with Nr. 112314 (POCI-01-0247-FEDER-112314).

References

[1] Cisco: 2020 CISO benchmark report, Comput. Fraud. Secur. 2020 (3) (2020) 4, https://doi.org/10.1016/S1361-3723(20)30026-9.

[2] ETSI, Human Factors (HF): QoE requirements for real-time communication services, ETSI Technical Report 102 643 1, 2009, pp. 1–37, http://www.etsi.org/deliver/etsi_tr/102600_102699/102643/01.00.01_60/tr_102643v010001p.pdf.

[3] W. Robitza, A. Ahmad, P.A. Kara, L. Atzori, M.G. Martini, A. Raake, L. Sun, Challenges of future multimedia QoE monitoring for internet service providers, Multimed. Tools Appl. 76 (21) (2017) 22243–22266, https://doi.org/10.1007/s11042-017-4870-z.

[4] K. Bouraqia, E. Sabir, M. Sadik, L. Ladid, Quality of experience for streaming services: measurements, challenges and insights, IEEE Access 8 (2020) 13341–13361, https://doi.org/10.1109/ACCESS.2020.2965099.

[5] R. Mahindra, H. Viswanathan, K. Sundaresan, M.Y. Arslan, S. Rangarajan, A practical traffic management system for integrated lte-wifi networks, in: Proceedings of the 20th Annual International Conference on Mobile Computing and Networking, MobiCom '14, Association for Computing Machinery, New York, NY, USA, 2014, pp. 189–200.

[6] U.P. Moravapalle, S. Sanadhya, A. Parate, K.H. Kim, Pulsar: improving throughput estimation in enterprise LTE small cells, in: Proceedings of the 11th ACM Conference on Emerging Networking Experiments and Technologies, CoNEXT 2015, 2015.

[7] B. Sas, K. Spaey, C. Blondia, A son function for steering users in multi-layer lte networks based on their mobility behaviour, in: 2015 IEEE 81st Vehicular Technology Conference (VTC Spring), 2015, pp. 1–7.

[8] V.O. Tikhvinskiy, G. Bochechka, Prospects and QoS requirements in 5G networks, J. Telecommun. Inf. Technol. 2015 (1) (2015) 23–26.

[9] I. Angelopoulos, E. Trouva, G. Xilouris, A monitoring framework for 5G service deployments, in: IEEE International Workshop on Computer Aided Modeling and Design of Communication Links and Networks, CAMAD 2017-June, 2017.

[10] N. Banović-Ćurguz, D. Ilišević, Mapping of qos/qoe in 5g networks, in: 2019 42nd International Convention on Information and Communication Technology, Electronics and Microelectronics (MIPRO), 2019, pp. 404–408.

[11] M.S. Mushtaq, S. Fowler, B. Augustin, A. Mellouk, Qoe in 5g cloud networks using multimedia services, in: 2016 IEEE Wireless Communications and Networking Conference, 2016, pp. 1–6.

[12] R. Dubin, R. Shalala, A. Dvir, O. Pele, O. Hadar, A fair server adaptation algorithm for HTTP adaptive streaming using video complexity, Multimed. Tools Appl. 78 (9) (2019) 11203–11222, https://doi.org/10.1007/s11042-018-6615-z.

[13] Q. Li, Understanding the causal impact of the video delivery throughput on user engagement, Multimed. Tools Appl. 78 (11) (2019) 15589–15604, https://doi.org/10.1007/s11042-018-7013-2.

[14] M.H. Mazhar, Z. Shafiq, Real-time video quality of experience monitoring for HTTPS and QUIC, in: Proceedings - IEEE INFOCOM 2018-April, 2018, pp. 1331–1339.

[15] K. Bouraqia, W. Attaoui, E. Sabir, Solving startup-delay-QoE dilemma for video streaming services in 5G networks, vol. 881, Springer International Publishing, 2019.

[16] J. Song, F. Yang, Y. Zhou, S. Wan, H.R. Wu, QoE evaluation of multimedia services based on audiovisual quality and user interest, IEEE Trans. Multimed. 18 (3) (2016) 444–457, https://doi.org/10.1109/TMM.2016.2520090.

[17] J. Nightingale, P. Salva-Garcia, J.M. Calero, Q. Wang, 5G-QoE: QoE modelling for ultra-HD video streaming in 5G networks, IEEE Trans. Broadcast. 64 (2) (2018) 621–634, https://doi.org/10.1109/TBC.2018.2816786.

[18] J.P. Lopez, D. Jimenez, J.A. Rodrigo, J.M. Menendez, F. Alvarez, N. Sanchez, J.M. Lalueza, Virtualized module for distributed quality assessment applied to video streaming in 5G networks environments, in: IEEE International Symposium on Broadband Multimedia Systems and Broadcasting, BMSB 2018-June, 2018.

[19] A. Bhargava, J. Martin, S.V. Babu, Comparative evaluation of user perceived quality assessment of design strategies for http-based adaptive streaming, ACM Trans. Appl. Percept. 16 (4) (2019), https://doi.org/10.1145/3345313.

[20] C. Qiao, J. Wang, Y. Liu, Beyond QoE: diversity adaption in video streaming at the edge, in: Proceedings - International Conference on Distributed Computing Systems 2019-July, 2019, pp. 317–326.

[21] B. Hou, J. Zhang, QoE estimation of DASH-based mobile video application using deep reinforcement learning, https://doi.org/10.1007/978-3-030-60239-0_43, 2020, pp. 633–645.

[22] A.O. El Meligy, M.S. Hassan, T. Landolsi, A buffer-based rate adaptation approach for video streaming over HTTP, in: Wireless Telecommunications Symposium 2020-April, 2020, pp. 1–5.

[23] P. Uthansakul, P. Anchuen, M. Uthansakul, A. Ahmad Khan, Estimating and synthesizing QoE based on QoS measurement for improving multimedia services on cellular networks using ANN Method, IEEE Trans. Netw. Serv. Manag. 17 (1) (2020) 389–402, https://doi.org/10.1109/TNSM.2019.2946091.

[24] I. Bartolec, I. Orsolic, L. Skorin-Kapov, Inclusion of end user playback-related interactions in YouTube video data collection and ML-based performance model training, in: 2020 12th International Conference on Quality of Multimedia Experience, QoMEX 2020, 2020.

[25] I. Orsolic, M. Seufert, On machine learning based video QoE estimation across different networks, in: Proceedings of the 16th International Conference on Telecommunications, ConTEL 2021, 2021, pp. 62–69.

[26] F. Laiche, A. Ben Letaifa, T. Aguili, QoE-aware traffic monitoring based on user behavior in video streaming services, in: Concurrency and Computation: Practice and Experience, May 2021, 2021, pp. 1–14.

[27] R.A. Aljiznawi, N.H. Alkhazaali, S.Q. Jabbar, D.J. Kadhim, Quality of service (qos) for 5g networks, Int. J. Future Comput. Commun. 6 (1) (2017) 27.

[28] D. Raca, J.J. Quinlan, A.H. Zahran, C.J. Sreenan, Beyond throughput: a 4g lte dataset with channel and context metrics, in: Proceedings of the 9th ACM Multimedia Systems Conference, MMSys '18, Association for Computing Machinery, New York, NY, USA, 2018, pp. 460–465.

[29] F. Dobrian, V. Sekar, A. Awan, I. Stoica, D. Joseph, A. Ganjam, J. Zhan, H. Zhang, Understanding the impact of video quality on user engagement, Comput. Commun. Rev. 41 (4) (2011) 362–373, https://doi.org/10.1145/2043164.2018478.

[30] S.S. Krishnan, R.K. Sitaraman, Video stream quality impacts viewer behavior: inferring causality using quasi-experimental designs, IEEE/ACM Trans. Netw. 21 (6) (2013) 2001–2014.

[31] A. Ahmed, Z. Shafiq, H. Bedi, A. Khakpour, Suffering from buffering? Detecting qoe impairments in live video streams, in: 2017 IEEE 25th International Conference on Network Protocols (ICNP), 2017, pp. 1–10.

[32] O. Oyman, S. Singh, Quality of experience for http adaptive streaming services, IEEE Commun. Mag. 50 (4) (2012) 20–27, https://doi.org/10.1109/MCOM.2012.6178830.

[33] T. Karagkioules, C. Concolato, D. Tsilimantos, S. Valentin, A comparative case study of HTTP adaptive streaming algorithms in mobile networks, in: Proceedings of the 27th Workshop on Network and Operating Systems Support for Digital Audio and Video, ACM, 2017.

[34] O. Ognenoski, M.M. Nasralla, M. Razaak, M. Martini, P. Amon, DASH-based video transmission over LTE networks, in: 2015 IEEE International Conference on Communication Workshop (ICCW), IEEE, 2015, pp. 1783–1787, http://ieeexplore.ieee.org/document/7247439/.

[35] H.Y. Weng, R.H. Hwang, C.F. Lai, Live MPEG-DASH video streaming cache management with cognitive mobile edge computing, J. Ambient Intell. Humaniz. Comput. (2020), https://doi.org/10.1007/s12652-020-02549-z.

[36] A. Salvador, J. Nogueira, S. Sargento, QoE assessment of HTTP adaptive video streaming, in: S. Mumtaz, J. Rodriguez, M. Katz, C. Wang, A. Nascimento (Eds.), Wireless Internet, in: Lecture Notes of the Institute for Computer Sciences, Social Informatics and Telecommunications Engineering, vol. 146, Springer International Publishing, Cham, 2015, pp. 235–242.

[37] K. Spiteri, R. Sitaraman, D. Sparacio, From theory to practice: improving bitrate adaptation in the dash reference player, in: Proceedings of the 9th ACM Multimedia Systems Conference, MMSys '18, Association for Computing Machinery, New York, NY, USA, 2018, pp. 123–137.